Soft Matter

Accepted Manuscript

This article can be cited before page numbers have been issued, to do this please use: Z. He, Y. Zhuo, F. Wang, J. He and Z. Zhang, *Soft Matter*, 2019, DOI: 10.1039/C9SM00024K.

ROYAL SOCIETY OF CHEMISTRY

rsc.li/soft-matter-journal

ROYAL SOCIETY OF CHEMISTRY View Article Online
DOI: 10.1039/C9SM00024K

Soft Matter

ARTICLE

Understanding the role of hollow sub-surface structures in reducing ice adhesion strength

Received 00th January 20xx,
Accepted 00th January 20xx

DOI: 10.1039/x0xx00000x

www.rsc.org/

Zhiwei He,[ab] Yizhi Zhuo,[b] Feng Wang,[b] Jianying He[b] and Zhiliang Zhang*[b]

The accretion of ice on exposed surfaces infers detrimental effects on many aspects of life and technology. Passive icephobic coatings, designed by strategies towards lowering ice adhesion to mitigate the icing problems, have recently received wide attention. In our previous studies, the incorporation of hollow sub-surface structures which act as macro-scale crack initiators has been shown to dratically lower the ice adhesion on PDMS surfaces. In this study, the effects of hollow sub-surface structure geometry, such as the heights, shapes, and distributions, as well as directions of the applied shear force, are experimentally investigated. Our results show that the number of potential macro-scale crack initiation sites dictates ice adhesion strength. Directions of the applied shear force also influence ice adhesion strength when the potential crack length is dependent on the applied shear force direction. The inter-locking effect between ice and the coating, caused by the pre-deformation, needs to be considered if one of the dimensions of the hollow sub-surface structures approaches millimeter scale. These results improve the understanding of the role of hollow sub-surface structures in reducing ice adhesion, providing new insights on the design principles for multi-scale crack initiators promoted icephobic surfaces.

Introduction

Reducing ice adhesion is an important strategy to mitigate ice accretion on exposed surfaces, such as power lines, wind turbines, aircraft and offshore platforms.[1-3] Various approaches towards lowering ice adhesion have been introduced, including superhydrophobic surfaces,[4-7] aqueous lubricating layers,[8-10] organic lubricating layers,[11-14] polyelectrolyte brush layers,[15-17] organogels,[18-21] and multi-scale crack initiators promoted icephobic surfaces.[22-25] Of these approaches, the macro-scale crack initiators promoted surfaces represent a promising alternative with great potential in further reducing ice adhesion strength for a given surface chemistry and texture.

Cracks often need to be avoided in structures and components for safety reasons,[26-28] while the formation of cracks at ice contact interface can facilitate the reduction of ice adhesion. Generally, ice adhesion strength can be estimated by the following equation:[23,24,29,30]

$$\tau_c = \sqrt{\frac{E^* G}{\pi a \Lambda}} \quad (1)$$

where E^* is the apparent elastic modulus, G is the surface energy, a is the length of the crack and Λ is a non-dimensional constant determined by the geometric configuration of the crack. It indicates that the ice adhesion strength can be reduced if the total crack length can be maximized. For a specific material surface with constant thickness, in general, there are three factors that influence the crack length and thus ice adhesion strength: (a) the number of crack initiation sites, (b) the length of an individual crack, and (c) the geometric configuration of cracks.

For a smooth surface without hollow sub-surface structures, crack initiations only appear at the edges of the ice cube during an ice adhesion test,[23] and the length of such initiation sites (potential crack length) can be ignored when the length of the ice cube is large. For a surface with hollow sub-surface structures, crack initiations appear at multiple locations where stress concentration occurs,[23,31] and the total length of these potential cracks can be described by the following equation:

$$\lim_{L\to\infty} \frac{\sum a_i}{L} = \text{constant} \quad (2)$$

where a_i is the individual crack length and L is the dimension of the ice cube. According to the equation (2), it is possible to create a large number of crack initiation sites for maximizing the total crack length,[23,32] where the number of crack initiation sites can be controlled by designing and tailoring of hollow sub-surface structures, including the shape, height and the distribution of hollow sub-surface structures.

The geometric configuration of the crack can influence crack formation and the path of crack propagation,[28] especially for elastic coatings with hollow sub-surface structures. Verma

[a] College of Materials and Environmental Engineering, Hangzhou Dianzi University, Hangzhou 310018, China
[b] NTNU Nanomechanical Lab, Department of Structural Engineering, Norwegian University of Science and Technology (NTNU), Trondheim 7491, Norway. E-mail: zhiliang.zhang@ntnu.no

et al. found that the crack propagated smoothly on a homogenous and smooth PDMS film, but on a PDMS film with hollow micro-channels, it became arrested at the vicinity of the channel.[32] The crack initiated again as the loading force became sufficiently high, and it propagated rather catastrophically until it became arrested close to the next channel.[32] We realize that the geometric configuration of the crack can be varied by changing directions of the applied shear force and optimizing of the shapes, the heights and the distributions of hollow sub-surface structures, which provides better understanding of the cracking mechanism on elastic icephobic coatings with hollow sub-surface structures.

To the best of our knowledge, there are few studies on the effect of these influencing factors on ice adhesion strength. Herein, we prepare polydimethylsiloxane (PDMS) coatings with three patterns of hollow sub-surface structures to understand their role in reducing ice adhesion strength, including the effect of hollow sub-surface structure geometry (e.g., height, shape and distribution) and directions of the applied shear force. We believe that the outcome of this study will facilitate the design of multi-scale cracks promoted icephobic surfaces.

Experimental

Materials. The sylgard®184 silicone elastomer kit (polydimethylsiloxane, PDMS) was purchased from the Dow Corning Corporation.

Preparation of SU8 patterns. The negative photoresists SU8-5 and SU8-2010 (MicroChem Corp., Newton, MA) were used to fabricate SU8 patterns via a photolithography process.[23] The spin-comating speeds for SU8-5 and SU8-2010 were chosen as 3000 rpm and 3500 rpm to obtain SU8 patterns with the heights of 5 μm and 10 μm, respectively. The design details of SU8 patterns are explained in the following figures.

Preparation of PDMS coatings with hollow sub-surface structures. The preparation of polydimethylsiloxane (PDMS) coatings with hollow sub-surface structures follows our previous study,[23] and the process is described in Figure 1. The mixture of PDMS prepolymer and a curing agent (weight ratio, 10:1) was stirred vigorously for 10 min and degassed to remove air bubbles for 40 min. It was then poured on a silicon wafer with SU8 pattern and spin-coated at a speed of 1400 rpm for 30 s to obtain a PDMS coating, followed by curing at 65 °C for 2 hours. The thickness of the as-prepared coating was measured as 67 μm by a contact stylus profilometer (Dektak 150, Veeco). Before peeling off from silicon wafer, PDMS coatings as well as glass substrates were treated with oxygen plasma (Femto plasma cleaner, 50% O_2 flow/80% power) for 12 s. Finally, the PDMS coating (67 μm) with sub-surface structures was carefully bonded on glass substrates and cured at 65 °C for another 2 hours. It should be noted that the thickness of all the coatings in this study is ~67 μm.

Ice adhesion test. Ice adhesion strength was characterized by using an Instron MicroTester (Instron®Model 5944) via a vertical shear test. The details of preparing ice cube samples and an ice adhesion test follow our previous studies.[3,23,24] Each sample was tested for three times, and the standard error was used for the tested data. Besides, there is no visible damage on PDMS surface after ice removal.

Results and discussion

The preparation route of polydimethylsiloxane (PDMS) coatings with macro-scale hollow sub-surface structures is illustrated in Figure 1. Three patterns (three types of SU8 templates, Figure 2) of PDMS coatings with macro-scale hollow sub-surface structures are investigated to understand the role of hollow sub-surface structures induced macro-cracks at the ice/solid interface in reducing ice adhesion strength (Figure 2-4). Ice adhesion strength of pure PDMS coating (67 μm) without macro-scale hollow sub-surface structures is characterized as 192.3±18.0 kPa and used as a reference in the following studies.

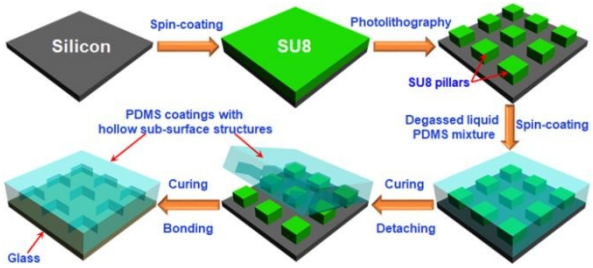

Figure 1 The representative route of the PDMS coating with hollow sub-surface structures. The layer thickness of the PDMS coating is ~67 μm.

In pattern 1, the dimension of macro-scale hollow sub-surface structure is 1 mm × 1 mm × 5 μm (or 10 μm), and the edge-to-edge spacing (*b* or *c*) is the same both in the *x* and *y* directions (Figure 2a). When the height of macro-scale hollow sub-surface structures is 5 μm, ice adhesion strength (the same in the *x* or *y* direction because of the symmetry of macro-scale hollow sub-surface structures) decreases from 152.6±15.1 kPa to 107.4±11.8 kPa when the edge-to-edge spacing (*b* or *c*) ranges from 3 mm to 1 mm (Figure 3), showing a reduction from 20.6% to 44.1% (Table 1), respectively. It indicates that the more macro-scale hollow sub-surface structures exist, the more macro-cracks can be induced and thus ice adhesion can be greatly reduced.

Table 1 The reduction ratio of ice adhesion on PDMS coatings with macro-scale hollow sub-surface structures

The reduction ratio of ice adhesion[a]		Directions of the applied force		
		x	45°	y
Pattern 1[b]	5 μm[c]	20.6-44.1%	28.1-57.8%	20.6-44.1%
	10 μm	27.0-53.5%	38.7-63.9%	27.0-53.5%
Pattern 2	5 μm	12.0-44.0%	4.60-33.6%	6.30-34.2%
	10 μm	19.0-53.5%	15.5-48.2%	12.4-45.1%
Pattern 3	5 μm	34.1-63.4%	28.5-59.5%	23.3-52.5%
	10 μm	32.2-61.8%	25.2-57.7%	15.0-45.2%

[a]The reduction ratio of ice adhesion when the edge-to-edge spacing (*c*) varies from 3 mm to 1 mm.

[b]The type of macro-scale hollow sub-surface structures.

[c]The height of macro-scale hollow sub-surface structures.

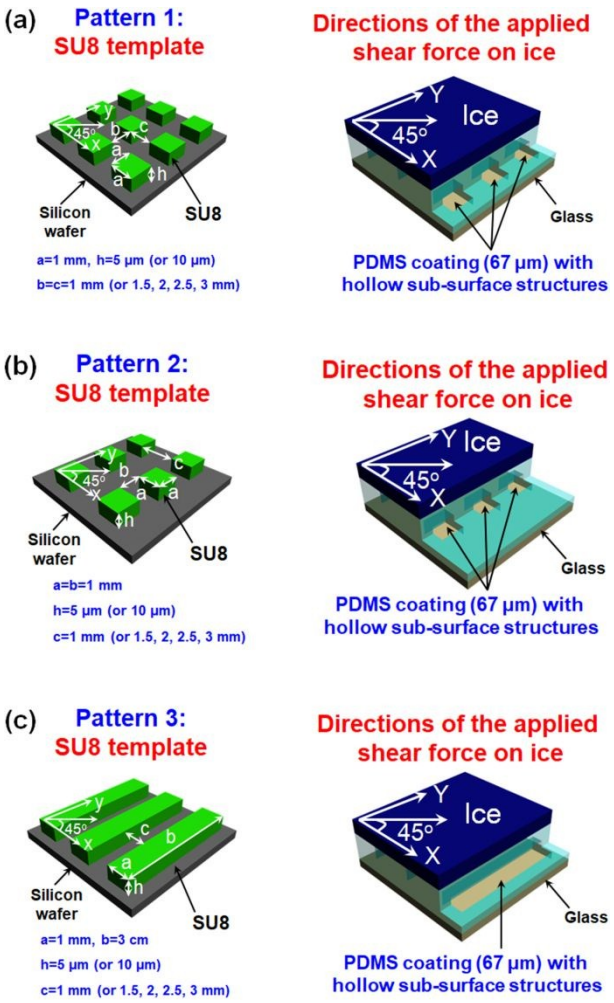

Figure 2 SU8 templates and directions of the applied shear force during an ice adhesion test for (a) pattern 1, (b) pattern 2 and (c) pattern 3. The height of macro-scale hollow sub-surface structures is 5 μm (or 10 μm), and directions of the applied shear force are in the *x*, *y* and 45° directions.

Interestingly, ice adhesion strength in the 45° direction is much smaller than that in the *x* or *y* direction as shown in Table 1 and Figure 3. It is clear from pattern 1 that the edge-to-edge spacing (*b* or *c*) and the number of potential crack initiation sites are the same for one specific coating, and the only difference is the direction of the applied shear force (Figure 2a). According to the equation (1), these results indicate that the total length of cracks or the geometric configuration of cracks along the applied shear force should be different if the directions of the applied shear force are changed. To understand the formation of cracks, a schematic overview is presented in Figure 4a. Actually, the maximum length (L_{max}) of an initiated crack in the 45° direction along the applied shear force is about 1.414 times as that in the *x* or *y* direction (Figure 4a), for the length of the diagonal line is as ~1.414 times as the length of a side. As a result, the ice adhesion strength along the applied shear force direction can be expected lower than the orthogonal directions. Therefore, for one specific coating with hollow sub-surface structures, ice adhesion strength can become the lowest as long as the total length of initiated cracks is biggest under different directions of the applied shear force.

When the height of hollow sub-surface structures increases to 10 μm in pattern 1, the ice adhesion strength is shown in Figure 3 (red and green bars) and the reduction ratio of ice adhesion can be seen in Table 1. For one specific coating, the directions of the applied shear force indeed influence ice adhesion strength in the same manner as 5 μm sub-surface structures (Table 1). To make the PDMS coating more deformable, the layer thickness over hollow sub-surface structures can be reduced by increasing the height of these hollow sub-surface structures. Thus, macro-cracks can be induced easily at the interface for the case with height of 10 μm rather than 5 μm during a shear test. As a result, ice adhesion strength for the case with height of 10 μm is lower than that for the case with height of 5 μm. This is because when the height of the sub-surface structures increases, it becomes easier to initiate cracks. In short, increasing the height of the hollow sub-surface structures can reduce the ice adhesion strength for pattern 1.

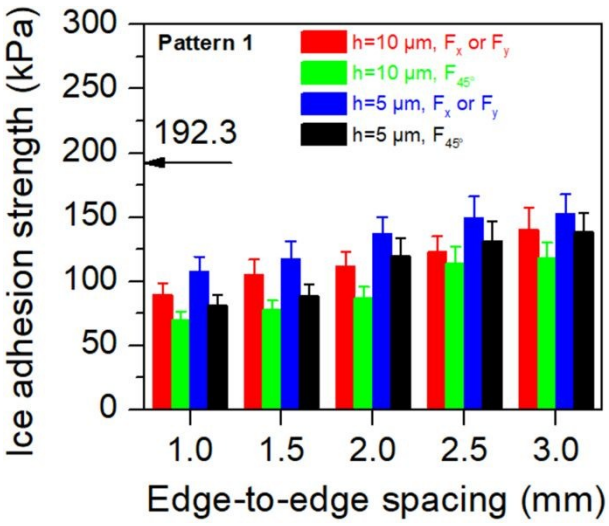

Figure 3 Ice adhesion strengths of PDMS coatings with macro-scale hollow sub-surface structures for pattern 1. The height of macro-scale hollow sub-surface structures is 5 μm (or 10 μm), and directions of the applied shear force are in the *x*, *y* and 45° directions.

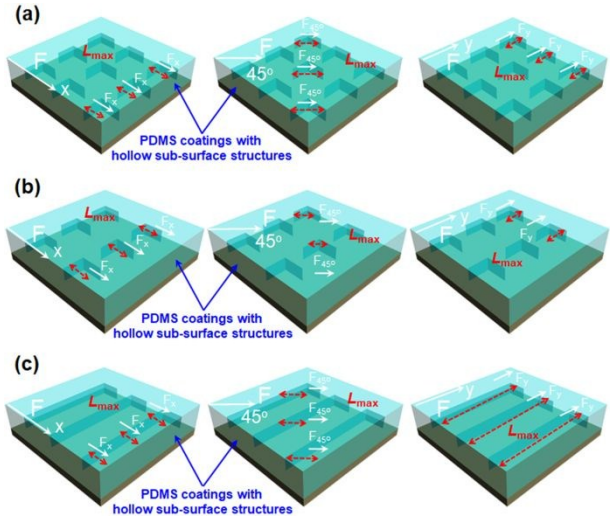

Figure 4 Schematic overview of the maximum length (L_{max}) of an initiated crack under the applied shear force in *x*, *y* and 45° directions for (a) pattern 1, (b) pattern 2 and (c) pattern 3.

In pattern 2, the geometry and size of the hollow sub-surface structures are the same with pattern 1, but the edge-to-edge spacing (*c*) only varies in the *x* direction from 3 mm to 1 mm. When the height of macro-scale hollow sub-surface structures is 5 μm, the ice adhesion strength is presented in Figure 5, and the reduction ratio of ice adhesion strength is shown in Table 1. As the edge-to-edge spacing (*c*) ranges from 3 mm to 1mm, ice adhesion strength decreases from 169.3±16.7 kPa to 107.4±11.8 kPa in the *x* direction, from 183.5±18.8 kPa to 127.6±13.1 kPa in the 45° direction and from 180.1±17.9 kPa to 126.4±13.2 kPa in the *y* direction, showing a reduction from 12.0% to 44.0%, from 4.6% to 33.6% and from 6.3% to 34.2%, respectively. In Figure 4b, it can be found that the maximum length (L_{max}) of an initiated crack is larger in the *x* or *y* direction than that in the 45° direction, resulting in their low ice adhesion. Meanwhile, the edge-to-edge spacing (*c*) along the applied force direction can be varied for different coatings under different loading scenarios, but it is kept constant for one specific coating when the applied force direction is changed. The formation of cracks becomes difficult as the edge-to-edge spacing (*c*) along the applied shear force increases (Figure 2b). This is the reason why ice adhesion strength in the *x* direction is lower than that in the *y* direction. Therefore, when designing low ice adhesion strength, the total length of an initiated crack along the applied shear force needs to be as long as possible.

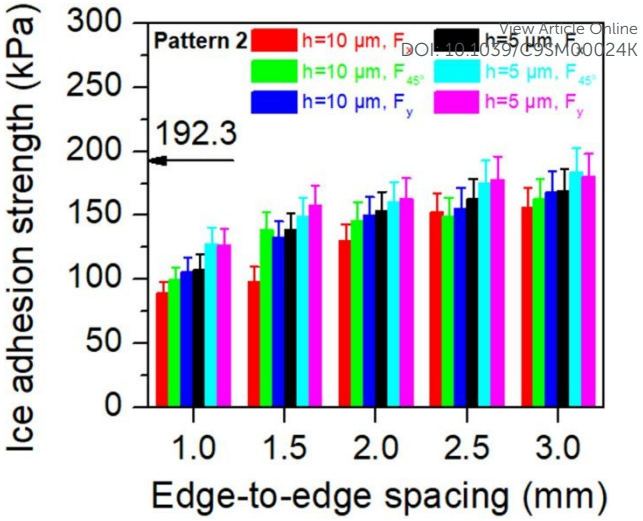

Figure 5 Ice adhesion strengths of PDMS coatings with macro-scale hollow sub-surface structures for pattern 2. The height of macro-scale hollow sub-surface structures is 5 μm (or 10 μm), and directions of the applied shear force are in the *x*, *y* and 45° directions.

Similar to pattern 1, the height of macro-scale hollow sub-surface structures in pattern 2 is selected as 10 μm to further study its influence on ice adhesion strength (Figure 5 and Table 1). It can be seen from Figure 5 that ice adhesion strength for the height of the hollow sub-surface structures of 10 μm (red, green and blue bars) is lower than that for 5 μm (black, cyan and pink bars), which is similar to the results for pattern 1. To summarize, we find that directions of the applied shear force, the height of macro-scale hollow sub-surface structures, the maximum length of an initiated crack and the edge-to-edge spacing influence ice adhesion strength for one specific coating.

Following the results of pattern 1 and pattern 2, we designed the dimension of macro-scale hollow sub-surface structures to be comparable with the dimension of the ice cube (Figure 2c) in pattern 3 in order to optimize the crack length. Compared with pattern 1 and pattern 2, the total length of potential cracks in pattern 3 is generally larger (Figure 4c) and thus the ice adhesion strength is much lower in pattern 3, indicating that the crack length depends on the design of patterns of macro-scale hollow sub-surface structures. It can be found in Figure 6 (black bar) that the lowest ice adhesion strength reaches at 70.3±7.1 kPa under the applied shear force in the *x* direction and shows the largest reduction of 63.4% compared with pure PDMS coatings without hollow sub-surface structures. In Figure 4c, the maximum length (L_{max}) of cracks appears in the *y* direction, whereas the shortest edge-to-edge spacing occurs in the *x* direction. L_{max} in pattern 3 is at centimeter scale and thus the inter-locking effect between ice and substrate cracks needs to be considered.[33-35] As a result, the shortest edge-to-edge spacing in the x direction facilitates the formation of cracks. L_{max} can facilitate the formation of cracks, but L_{max} caused inter-locking of cracks also inhibits the formation of cracks.

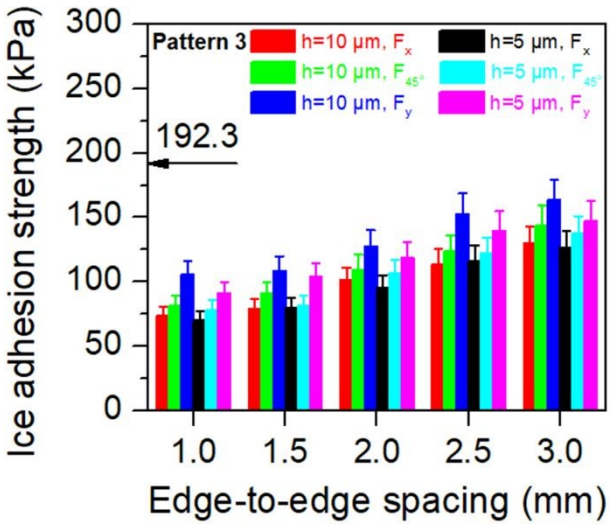

Figure 6 Ice adhesion strengths of PDMS coatings with macro-scale hollow sub-surface structures for pattern 3. The height of macro-scale hollow sub-surface structures is 5 μm (or 10 μm), and directions of the applied shear force are in the *x*, *y* and 45° directions.

We seek to understand whether ice adhesion strength can be further reduced if the height of the sub-surface structures increases as 10 μm. Surprisingly, ice adhesion strength shows an increasing trend for most of PDMS coatings when the height of macro-scale hollow sub-surface structures increase from 5 μm to 10 μm, which is opposite to the results for pattern 1 and pattern 2. This is because the deformation of water before freezing on the PDMS coating (pattern 1 and pattern 2) is not significant as the macro-scale hollow sub-surface structures is at millimeter scale (1 mm) (Figure 7a), while it (pattern 3) becomes evident as the macro-scale hollow sub-surface structures is comparable with the dimension of the ice cube at centimeter scale (3 cm) as illustrated in Figure 7b. When water becomes ice, the inter-locking effect between ice and the coating occurs and thus results in the increase of ice adhesion strength (Figure 7b).[34-36] For PDMS coatings (the height of macro-scale hollow sub-surface structures is 10 μm), the sub-surface structures have a competitive effect. On one hand, hollow sub-surface structures contribute to the reduction of ice adhesion, while on the other hand, the inter-locking increases the ice adhesion strength due to ice induced pre-deformation over hollow sub-surface structures. This is why ice adhesion strength (red, green and blue bars) of PDMS coating with the height of sub-surface structures (10 μm) is even higher than that of PDMS coating with the height of sub-surface structures (5 μm) (black bar). Therefore, when designing icephobic coatings with sub-surface structures, the inter-locking effect should be considered if the length of hollow sub-surface structures is comparable with that of ice cube.

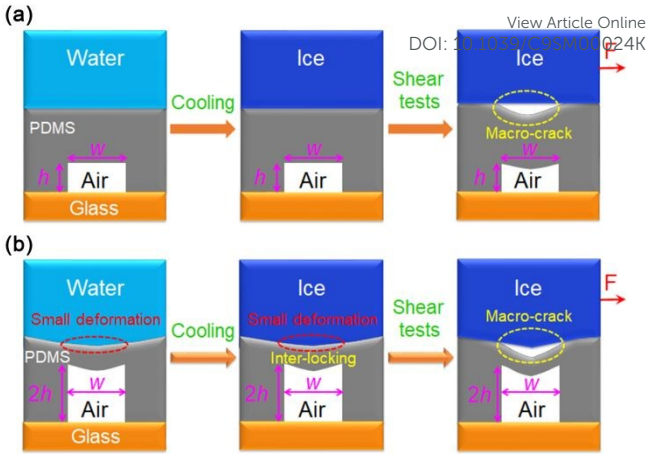

Figure 7 Possible behaviors of macro-scale hollow sub-surface structures with different heights during an ice adhesion test. The purpose of this schematic overview is only to illustrate possible inter-locking effect on surfaces with macro-scale hollow sub-surface structures when the height of hollow sub-surface structures increases in (b). *h* is at nano-scale and *w* is at macro-scale. Macro-cracks in (b) can be induced if the inter-locked ice is detached from the coating first. Of course, small deformation of macro-scale hollow sub-surface structures may exist in (a). Such inter-locking effect is not obvious when the width and length of hollow sub-surface structures are comparable (about 1 mm).

Conclusions

In this study, we designed three patterns with hollow sub-surface structures in PDMS coatings and investigated the role of macro-scale hollow sub-surface structures in reducing ice adhesion strength. Our results show that the number of potential crack initiation sites dictates ice adhesion strength. Directions of the applied shear force can influence ice adhesion strength if the maximum length of an initiated crack is different. The deformation-induced inter-locking effect between ice and the coating also needs to be considered if macro-scale hollow sub-surface structures are very large in one dimension (several millimeters). Our results improve the understanding on the effect of the geometrical factors of the hollow sub-surface structures on ice adhesion, and provide new insights on the design of multi-scale crack initiator promoted icephobic surfaces. However, either theoretical model or empirical equations are still needed for understanding the above strategy towards the design of low ice adhesion surfaces. Future work can be focused on finite element analysis based simulations to establish quantitative relationships for optimal surface design.

Conflicts of interest

There are no conflicts to declare.

Acknowledgements

The Research Council of Norway is acknowledged for the support to the FRINATEK project Towards Design of Super-Low Ice Adhesion Surfaces (SLICE, 250990) and the support to the Norwegian Micro- and Nano-Fabrication Facility, NorFab (245963). The National Natural Science Foundation of China (Grant No. 51803043) and the Science Foundation of Hangzhou Dianzi University (KYS205618119) are appreciated for the financial support.

Notes and references

1. A. J. Meuler, J. D. Smith, K. K. Varanasi, J. M. Mabry, G. H. McKinley and R. E. Cohen, *ACS Appl. Mater. Interfaces*, 2010, **2**, 3100-3110.
2. L. Bao, Z. Huang, N. V. Priezjev, S. Chen, K. Luo and H. Hu, *Appl. Surf. Sci.*, 2018, **437**, 202-208.
3. Z. He, E. T. Vågenes, C. Delabahan, J. He and Z. Zhang, *Sci. Rep.*, 2017, **7**, 42181.
4. S. Bengaluru Subramanyam, V. Kondrashov, J. Rühe and K. K. Varanasi, *ACS Appl. Mater. Interfaces*, 2016, **8**, 12583-12587.
5. T. Bharathidasan, S. V. Kumar, M. S. Bobji, R. P. S. Chakradhar and B. J. Basu, *Appl. Surf. Sci.*, 2014, **314**, 241-250.
6. L. Cao, A. K. Jones, V. K. Sikka, J. Wu and D. Gao, *Langmuir*, 2009, **25**, 12444-12448.
7. M. He, J. Wang, H. Li and Y. Song, *Soft Matter*, 2011, **7**, 3993-4000.
8. J. Chen, Z. Luo, Q. Fan, J. Lv and J. Wang, *Small*, 2014, **10**, 4693-4699.
9. J. Chen, R. Dou, D. Cui, Q. Zhang, Y. Zhang, F. Xu, X. Zhou, J. Wang, Y. Song and L. Jiang, *ACS Appl. Mater. Interfaces*, 2013, **5**, 4026-4030.
10. D. Chen, M. D. Gelenter, M. Hong, R. E. Cohen and G. H. McKinley, *ACS Appl. Mater. Interfaces*, 2017, **9**, 4202-4214.
11. T.-S. Wong, S. H. Kang, S. K. Y. Tang, E. J. Smythe, B. D. Hatton, A. Grinthal and J. Aizenberg, *Nature*, 2011, **477**, 443-447.
12. Y. Zhuo, F. Wang, S. Xiao, J. He and Z. Zhang, *ACS Omega*, 2018, **3**, 10139-10144.
13. K. Golovin and A. Tuteja, *Sci. Adv.*, 2017, **3**, e1701617.
14. F. Wang, W. Ding, J. He and Z. Zhang, *Chem. Eng. J.*, 2019, **360**, 243-249.
15. S. Chernyy, M. Järn, K. Shimizu, A. Swerin, S. U. Pedersen, K. Daasbjerg, L. Makkonen, P. Claesson and J. Iruthayaraj, *ACS Appl. Mater. Interfaces*, 2014, **6**, 6487-6496.
16. M. Ezzat and C.-J. Huang, *RSC Adv.*, 2016, **6**, 61695-61702.
17. Z. Liu, Z. He, J. Lv, Y. Jin, S. Wu, G. Liu, F. Zhou and J. Wang, *RSC Adv.*, 2017, **7**, 840-844.
18. D. L. Beemer, W. Wang and A. K. Kota, *J. Mater. Chem. A*, 2016, **4**, 18253-18258.
19. C. Urata, G. J. Dunderdale, M. W. England and A. Hozumi, *J. Mater. Chem. A*, 2015, **3**, 12626-12630.
20. Y. Wang, X. Yao, J. Chen, Z. He, J. Liu, Q. Li, J. Wang and L. Jiang, *Sci. China Mater.*, 2015, **58**, 559-565.
21. Y. Zhuo, V. Hakonsen, Z. He, S. Xiao, J. He and Z. Zhang, *ACS Appl. Mater. Interfaces*, 2018, **10**, 11972-11978.
22. E. J. Y. Ling, V. Uong, J.-S. Renault-Crispo, A.-M. Kietzig and P. Servio, *ACS Appl. Mater. Interfaces*, 2016, **8**, 8789-8800.
23. Z. He, S. Xiao, H. Gao, J. He and Z. Zhang, *Soft Matter*, 2017, **13**, 6562-6568.
24. Z. He, Y. Zhuo, J. He and Z. Zhang, *Soft Matter*, 2018, **14**, 4846-4851.
25. T. K. Chen, Q. Cong, Y. Li, J. F. Jin and K. L. Choy, *Cold Reg. Sci. Technol.*, 2018, **146**, 122-126.
26. Z. L. Zhang, C. Thaulow and M. Hauge, *Eng. Fract. Mech.*, 1997, **57**, 653-664.
27. J. Xu, Z. L. Zhang, E. Østby, B. Nyhus and D. B. Sun, *Int. J. Pres. Ves. Pip.*, 2009, **86**, 787-797.
28. A. Livne, E. Bouchbinder, I. Svetlizky and J. Fineberg, *Science*, 2010, **327**, 1359-1363.
29. M. Nosonovsky and V. Hejazi, *ACS Nano*, 2012, **6**, 8488-8491.
30. H. Yao and H. Gao, *J. Comput. Theor. Nanos.*, 2010, **7**, 1299-1305.
31. A. Majumder, A. Ghatak and A. Sharma, *Science*, 2007, **318**, 258-261.
32. M. K. S. Verma, A. Majumder and A. Ghatak, *Langmuir*, 2006, **22**, 10291-10295.
33. S. Yang, Q. Xia, L. Zhu, J. Xue, Q. Wang and Q.-m. Chen, *Appl. Surf. Sci.*, 2011, **257**, 4956-4962.
34. J. Chen, J. Liu, M. He, K. Li, D. Cui, Q. Zhang, X. Zeng, Y. Zhang, J. Wang and Y. Song, *Appl. Phys. Lett.*, 2012, **101**, 111603.
35. X. Li, Y. Zhao, H. Li and X. Yuan, *Appl. Surf. Sci.*, 2014, **316**, 222-231.
36. N. P. Mitchell, V. Koning, V. Vitelli and William T. M. Irvine, *Nat. Mater.*, 2016, **16**, 89.

View Article Online DOI: 10.1039/C9SM00024K

View Article Online
DOI: 10.1039/C9SM00024K

Table of Contents

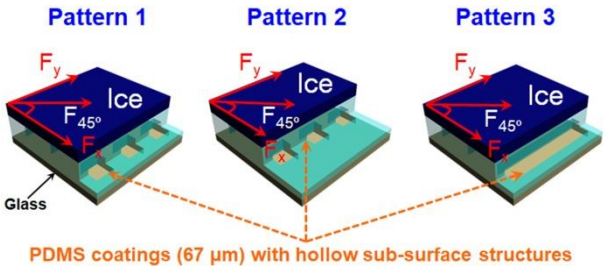

Polydimethylsiloxane coatings with three patterns of hollow sub-surface structures were prepared to understand their role in reducing ice adhesion strength.